

# Parting gravity's tail: quadrupole tails at fifth order and beyond via integer partitions

---

Alex Edison 

*Department of Physics and Astronomy, Northwestern University, Evanston, Illinois, 60208, USA*

*E-mail:* [alexander.edison@northwestern.edu](mailto:alexander.edison@northwestern.edu)

ABSTRACT: This work studies the systematic organization of higher-order gravitational quadrupole tails using generalized unitarity methods imported from the study of scattering amplitudes. The first major result is a constructive algorithm for generic arbitrary-order tail effective actions which links the structure of their loop integral basis expansion with integer partitions, and predicts that only a single new unitarity cut needs to be evaluated at each tail order with all other contributions given in terms of lower-loop data. The algorithm is employed to compute the tail-of-tail-of-tail-of-tail-of-tail ( $T^5$ ) contributions to the effective action and associated energy loss to gravitational waves. Validation of the new effective action and radiated energy is done through counterterm extraction and renormalization analysis, leading to complete agreement with known counterterms and renormalization flow equations.

---

## Contents

<b>1</b>	<b>Introduction</b>	<b>1</b>
<b>2</b>	<b>Review</b>	<b>2</b>
<b>3</b>	<b>Conjectured iterative tail construction</b>	<b>6</b>
<b>4</b>	<b>Construction of tail-of-tail-of-tail-of-tail-of-tail (<math>T^5</math>)</b>	<b>9</b>
<b>5</b>	<b>Radiated energy and renormalization of the quadrupole coupling</b>	<b>14</b>
<b>6</b>	<b>Conclusion</b>	<b>16</b>
<b>A</b>	<b>Integrals</b>	<b>18</b>

---

## 1 Introduction

Gravitational waves and their sources hold a large and pressing interest for both phenomenological and theoretical study. The LIGO-VIRGO-KAGRA network [1–3] demands more-precise predictions to inform template models, and pursuing this theoretical precision has exposed a host of conceptual and technical questions.

The best-explored framework to understand gravitational waves and their binary inspiral sources is the post-Newtonian approximation of general relativity (GR). In this approximation, the objects under consideration are *slowly moving* and *weakly gravitationally interacting*, which matches well with the expected behavior of a quasi-circular inspiral phase of binary black hole systems. The effective theory is well-studied through both classical perturbation theory [4–6] and Lagrangian descriptions manifesting the relevant degrees of freedom [7–12]. Within this effective field theory perspective, the non-linear dynamics of gravity lead to subtle phenomena known as “hereditary effects” [13] or “tails” [14], which account for the interaction between the residual binding-potential modes of the gravitational field, and the radiative modes. The tails importantly lead to corrections to the radiated energy of a binary black hole system, and also result in *non-local-in-time* evolution [13]. This induced history dependence of the system complicates the connection between scattering and bound systems at subleading perturbative orders [15–18].

In Refs. [19, 20], the current author and Levi studied higher-order tail effects using generalized unitarity methods. These techniques, originally developed for the study of scattering amplitudes in particle physics, allow for the construction of observables using simple, gauge invariant building blocks. They allowed access to the tail-of-tail-of-tail-of-tail ( $T^4$ ), the most

advanced tail ever computed for generic quadrupoles; traditional field theory techniques have achieved  $T^3$  [21], while further orders have been computed using the “self-force” framework, which is limited to an analytic expansion in the binary mass ratio [22–25]. Additionally, generalized unitarity methods naturally organized the results in a way that highlighted recurring patterns between tail orders. The current work builds on the success of Refs. [19, 20] by identifying a combinatoric organization of the generalized unitarity decomposition of all currently known tails. This systematic solution reduces the difficulty of constructing new tail orders to evaluating a single new unitarity cut diagram at each loop order; all of the rest of the needed information is recycled from previous orders.

The structure of the paper is as follows. Section 2 briefly reviews the setup of the problem: the composite-particle EFT, in-in formalism for dissipative actions, and unitarity-based methods. Next, section 3 introduces a computation method for arbitrary-order tails. The method associates the iterative structure of the effective action to permutations of integer partitions, and exactly reproduces all of the results of [20]. This novel method is deployed in section 4 to streamline the computation of the tail-of-tail-of-tail-of-tail-of-tail ( $T^5$ ) effective action, eq. (4.28). Section 5 covers the extraction of inclusive energy loss, incorporating the new correction from  $T^5$ , eq. (5.6), as well as verifying the renormalization group flow of the quadrupole coupling. A short summary of the integrals needed for  $T^5$  is given in appendix A.

## 2 Review

Many aspects of the current work build directly on Refs. [19, 20]. As such, we will limit the current review to a brief recap of the necessary terminology and symbols and direct interested readers to Ref. [20] for a more pedagogical discussion and contextual references.

We start from the post-Newtonian (PN) effective field theory of general relativity [7, 26, 27], in which the objects under consideration are *slow moving* and *weakly interacting*. Under these assumptions, we have two perturbative quantities – the (relative) velocity of the objects and their potential, governed by Newton’s Constant – which for quasi-circular orbits can be related via the virial theorem

$$v^2 \sim \frac{G_N m}{r} \ll 1, \quad (2.1)$$

and can approximately separate the graviton into near zone modes (which account for binding potentials between objects), and far zone (radiation) modes. However, the nonlinear nature of gravity leads to non-trivial interference phenomena that occur at subleading orders in perturbation theory. The lowest-order such effect that contributes corrections to gravitational radiation is the *quadrupole tail*, in which gravitational radiation sourced from a quadrupole interacts one (or more) times with a background gravitational potential.

From an effective field theory perspective, we study these effects by considering an effective theory for post-Newtonian gravity coupled to a *composite particle* which admits a spatial

multipole expansion [26, 28–31]

$$S_{\text{eff}}[g_{\mu\nu}, y^\mu, e_A^\mu] = -\frac{1}{16\pi G} \int d^4x \sqrt{-g} R[g_{\mu\nu}] + S_{\text{matter}}[g_{\mu\nu}(y), y^\mu, e_A^\mu] \quad (2.2)$$

$$S_{\text{matter}}[g_{\mu\nu}(y), y^\mu, e_A^\mu] = - \int dt \sqrt{g_{00}} \left[ E(t) - I^{ij}(t) \mathcal{E}_{ij} + \text{others} \right]. \quad (2.3)$$

where  $E(t)$  is the gravitating energy of the system,  $\mathcal{E}_{ij}$  is the even-parity projection of the curvature tensor,  $I^{ij}(t)$  a time-dependent charge-type quadrupole, and “others” refers to related sources that lead to interference effects like the “failed tail” [32], higher-order-multipole tails [33], and current-type tails, which we will not explore here.  $y^\mu$  and  $e_A^\mu$  are the matter (binary-as-point-particle) coordinate and associated tetrad, respectively; they are necessary for the formal definition of the EFT, but will play no direct role in the following computations. From this starting theory, we integrate out the interaction of the quadrupole with gravity, which will produce an effective action describing the potentially *non-local-in-time* evolution of the quadrupole (in frequency space) [4, 34–36]:

$$S_{\text{eff}}^{\text{tails}} = \int d\omega f(\omega) \underbrace{I^{ij}(\omega) I_{ij}(-\omega)}_{\kappa(\omega)}. \quad (2.4)$$

Because these effects contain dissipative (and thus time-asymmetric) contributions [13, 14], it is necessary to employ an “in-in” or “closed time path” (CTP) formalism to recover the correct causal behavior of the system [34, 36–39]. The CTP prescription is rather simple for the tails:

- We associate a “history label” in  $\{+, -\}$  to each of the quadrupoles taking part in the tail:  $I^{ij}(\omega) \rightarrow I_{\pm}^{ij}(\omega) \Rightarrow \kappa(\omega) \rightarrow \kappa_{\pm\mp}(\omega)$ ;
- All radiation-mode graviton propagators use causal (advanced/retarded)  $i0$  prescriptions in Fourier space according to which history labels they are connected to:

$$G_{-+ / +-}(x - x') = G_{\text{ret/adv}}(x - x') = \int \frac{d^D p}{(2\pi)^D} \frac{e^{-ip_\mu(x-x')^\mu}}{(p^0 \pm i0)^2 - |\vec{p}|^2}. \quad (2.5)$$

Note that we will employ dimensional regularization as our regularization scheme, where  $D$  will denote the analytically continued number of spacetime dimensions, and  $d = D - 1$  the spatial dimensions;

- Momentum conservation implies there is only one frequency in the tails problem. Thus, for each diagram we sum over taking all radiation propagators to be retarded, then all advanced;
- The sum over propagator types leads to a modified  $f(\omega)$  from eq. (2.4) with both  $\omega$ -even  $\rightarrow$  *conservative* terms and  $\omega$ -odd  $\rightarrow$  *dissipative* terms

$$S_{\text{CTP}}^{\text{tails}} = \frac{1}{2} \int d\omega [f_{\text{even}}(\omega)(\kappa_{-+}(\omega) + \kappa_{+-}(\omega)) + f_{\text{odd}}(\omega)(\kappa_{-+}(\omega) - \kappa_{+-}(\omega))]. \quad (2.6)$$

The CTP prescription has associated extensions to Noether's theorem, which we will employ in section 5.

We can organize the computation of the tail effective action, eq. (2.4), using generalized unitarity methods. First, we striate the effective action according to the loop order of diagrams that contribute (or, equivalently, the naive powers of  $G_N E$ ), which we refer to as  $S_{T^n}$ . Each of these loop orders is then further decomposed into a basis of Euclidean loop momentum integrals,  $\mathcal{I}_i$ , with  $d$ - and  $\omega$ -dependent coefficients

$$S_{T^n} = \int d\omega \sum_{\substack{i \text{ in} \\ \text{integral basis}}} c_i(d, \omega, I^{ij}(\omega)) \mathcal{I}_i, \quad (2.7)$$

where all of the  $i0$  prescription choices contribute through the analytic continuation of the results of the loop integrals. The coefficients in this basis are computable via generalized unitarity cuts [40–48]

$$\text{Cut}_G = \sum_{\substack{\text{states along} \\ \text{edges of } G}} \prod_{\substack{v \in \text{vertices} \\ \text{of } G}} \mathcal{A}_{\text{tree}}(v), \quad (2.8)$$

where  $G$  is a graph relevant to the problem. For gravitons, the sum over states acting on a pair of graviton polarization tensors  $\varepsilon_k^{\mu\nu}$  with associated momentum  $k$  is implemented by the physical state projector

$$\sum_{\text{states}} \varepsilon_k^{\mu\nu} \varepsilon_k^{\alpha\beta} \equiv \mathcal{P}_k^{\mu\nu; \alpha\beta} = \frac{1}{2} \left( P_k^{\mu\alpha} P_k^{\nu\beta} + P_k^{\mu\beta} P_k^{\nu\alpha} - \frac{2}{D-2} P_k^{\mu\nu} P_k^{\alpha\beta} \right), \quad (2.9)$$

$$P_k^{\mu\nu} \equiv \eta^{\mu\nu} - \frac{k^\mu q^\nu + k^\nu q^\mu}{k \cdot q}, \quad (2.10)$$

in which  $q^\mu$  is a null reference vector that will drop out of eq. (2.8). In the case of tails, the amplitudes we care about are:

- The quadrupole source amplitude for producing radiation gravitons,

$$\begin{aligned} \mathcal{M}_{Ig} &= \lambda_I I^{ij}(\omega) (\omega_g k_g^i \varepsilon_g^0 \varepsilon_g^j + \omega_g k_g^j \varepsilon_g^0 \varepsilon_g^i - k_g^i k_g^j \varepsilon_g^0 \varepsilon_g^0 - \omega_g^2 \varepsilon_g^i \varepsilon_g^j) \\ &\equiv \lambda_I J_I^{\mu\nu} \varepsilon_{\mu\nu} \\ &= I^{ij} \text{---}\varkappa\varkappa\varkappa\varkappa\varepsilon_{\mu\nu}, \end{aligned} \quad (2.11)$$

with coupling constant  $\lambda_I$ ,  $k_g$  and  $\varepsilon_g$  the momentum and polarization of the emitted graviton, and  $p_I$  the momentum of the quadrupole which we take to be the largest scale in the problem, and will evaluate in its rest frame *after* unitarity state sewing.

- The single potential-mode source amplitude (analogous to a graviton coupled to a world-line [49])

$$\mathcal{M}_{Eg} = \mathcal{M}_{sgs} = \frac{\lambda_E}{m_I^2} p_I^\mu p_I^\nu \varepsilon_{\mu\nu} = E \text{---}\varkappa\varkappa\varkappa\varepsilon_{\mu\nu}, \quad (2.12)$$



factor

$$\text{Cut}_G \xrightarrow[\text{tens. red.}]{\text{IBPs}} \overline{\text{Cut}}_G \mathcal{I}_G, \quad \frac{\overline{\text{Cut}}_G}{|G|} \mathcal{I}_G = \sum_{\substack{\mathcal{I}_i \text{ has propagators} \\ \text{compatible with } G}} c_i \mathcal{I}_i, \quad (2.16)$$

where  $|G|$  is the size of the automorphism group of the graph.

We will retain the tail symmetry convention from Ref. [20] where we sum over using both the advanced and retarded propagator in the CTP evaluation, but include a factor of 2 as a reflection symmetry factor *even for graphs that naively do not have this symmetry*.

### 3 Conjectured iterative tail construction

Ref. [20] demonstrated how generalized unitarity methods could be efficiently applied to the case of tail effective actions. In that work, the minimal loop integral basis was identified via careful analysis of possible diagram topologies. Then, the corresponding basis coefficients were computed using generalized unitarity cuts to sew together appropriate gravity amplitudes. It was observed that many of the coefficients present in  $T^4$  factorized into lower-loop-order structures, as did the integral basis itself.

In order to manifest these observed factorization patterns, we propose the following algorithm for constructing arbitrary tail orders ( $T^n$ ) organized as they would be according to generalized unitarity methods. First, we construct the basis of cut diagrams that contribute:

1. Enumerate the integer partitions of  $n$  into  $1, \dots, n$ :

$$\mathfrak{p}_n = \left\{ \{x_1, \dots\} \mid \sum_i x_i = n \text{ and } x_i \in \mathbb{Z} \text{ and } 1 \leq x_i \leq n \text{ and } x_i > x_{i+1} \right\} \quad (3.1)$$

2. Find all nonequivalent permutations of the partitions, which we will call  $\mathfrak{s}_n$
3. For each  $\sigma \in \mathfrak{s}_n$  construct the cut diagram  $G_\sigma$ :
  - (a) Read the elements in  $\sigma$  from left to right and insert
    - A source contact, eq. (2.13), for each  $x_i = 1$ ;
    - A bulk graviton contact  $\mathcal{M}_{x_i}$ , eq. (2.14), for each  $x_i > 1$ , with cut propagators connected to  $x_i - 2$  simple potential sources, eq. (2.12);
    - A cut propagator for between each sequential element, eq. (2.9);
  - (b) Complete the cut diagram by inserting a quadrupole  $I^{ij}(\omega_1)$  connected by a cut propagator to the first element, and a  $I^{mn}(\omega_2)$  connected by a cut propagator to the final element. Note that momentum conservation implies  $\omega_1 = -\omega_2$ .

For example, the leading tail has  $n = 1$ , for which  $\mathfrak{s}_1 = \{\{1\}\}$ . Step 3(a) tells us this necessitates inserting a source contact, which is connected on either side to a quadrupole:

$$\{1\} \Rightarrow \begin{array}{c} I^{mn} \blacksquare \\ \text{---} \\ E \bullet \\ \text{---} \\ I^{ij} \blacksquare \end{array} . \quad (3.2)$$

Similarly, for  $T^2$  we have  $\mathfrak{s}_2 = \{\{2\}, \{1, 1\}\}$ , leading to the cut diagrams

$$\{1, 1\} \Rightarrow \begin{array}{c} I^{mn} \blacksquare \\ \text{---} \\ E \bullet \\ \text{---} \\ E \bullet \\ \text{---} \\ I^{ij} \blacksquare \end{array} , \quad \{2\} \Rightarrow \begin{array}{c} I^{mn} \blacksquare \\ \text{---} \\ E \bullet \\ \text{---} \\ E \bullet \\ \text{---} \\ I^{ij} \blacksquare \end{array} \mathcal{M}_4 . \quad (3.3)$$

Further examples will be provided for  $T^5$  below.

The reduced unitarity cut coefficients for these basis diagrams – normally computed via eq. (2.16) or through reductions of Feynman diagrams – factorize based on the integer partition, and are given by

$$\overline{\text{Cut}}_{G_\sigma} = \mathcal{R} \prod_{x_i \in \sigma} \mathcal{T}_{x_i} \quad (3.4)$$

where  $\mathcal{R}$  is the radiation-reaction coefficient given below, and the  $\mathcal{T}_i$  will first appear in the computation of  $T^i$ , but can then be recycled for higher loop orders. From all of the cut coefficients computed in Ref. [20], we can identify the functions needed up through  $\mathcal{T}_4$  as

$$\mathcal{R} = \omega^4 \frac{(d+1)(d-2)}{(d+2)(d-1)}, \quad \mathcal{D}_3 = (d-3)(d-1)(d+1), \quad \mathcal{D}_1 = (d-1)d(d+1), \quad (3.5a)$$

$$\mathcal{T}_1 = -\frac{\mathcal{P}_4}{2d\mathcal{D}_3}, \quad (3.5b)$$

$$\mathcal{T}_2 = \frac{\omega^2(2d-3)\mathcal{P}_8}{3\mathcal{D}_3\mathcal{D}_1(d-2)(3d-2)(3d-4)}, \quad (3.5c)$$

$$\mathcal{T}_3 = \frac{\omega^2(3d-5)\mathcal{P}_{11}}{2\mathcal{D}_3^2\mathcal{D}_1(2d-3)(3d-2)(3d-4)}, \quad (3.5d)$$

$$\mathcal{T}_4 = \frac{\omega^2\mathcal{P}_{22}}{30\mathcal{D}_3^3\mathcal{D}_1(d-2)^2d(2d-3)(3d-2)^2(3d-4)^2(5d-6)(5d-8)}, \quad (3.5e)$$



with the numerator polynomials  $\mathcal{P}_x$  given by

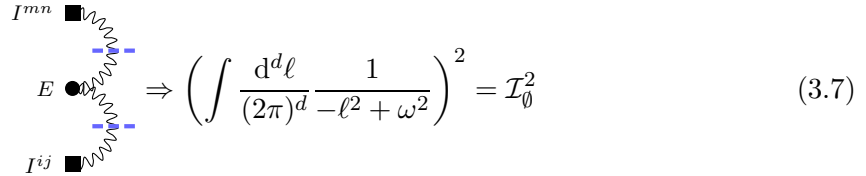
$$\mathcal{P}_4 = 12 - 2d + 5^2 - 4d^3 + d^4, \quad (3.6a)$$

$$\mathcal{P}_8 = 960 - 1696d + 424d^2 - 476d^3 + 330d^4 - 39d^5 + 53d^6 - 45d^7 + 9d^8, \quad (3.6b)$$

$$\begin{aligned} \mathcal{P}_{11} = & -3024 + 3720d + 2980d^2 + 996d^3 - 2426d^4 - 737d^5 + 799d^6 - 284d^7 - 36d^8 \\ & + 223d^9 - 117d^{10} + 18d^{11}, \end{aligned} \quad (3.6c)$$

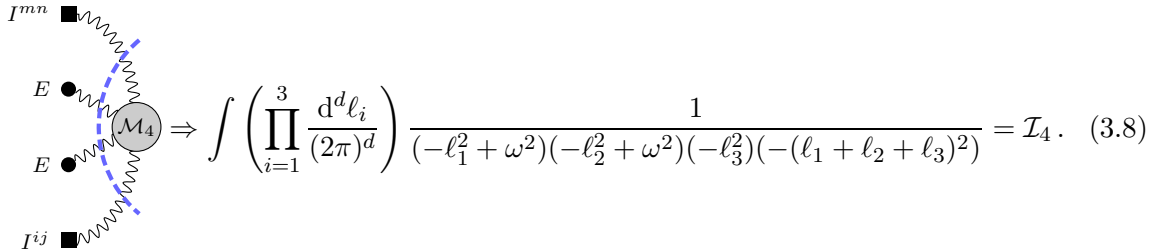
$$\begin{aligned} \mathcal{P}_{22} = & -60914073600 + 447389982720d - 1430856658944d^2 + 2688616654848d^3 \\ & - 3454174264320d^4 + 3432661203456d^5 - 2911608239232d^6 + 2203112130496d^7 \\ & - 1503589473248d^8 + 944837229872d^9 - 555238832200d^{10} + 309327324244d^{11} \\ & - 174143104426d^{12} + 101573518519d^{13} - 53485147433d^{14} + 21042703665d^{15} \\ & - 4908635433d^{16} + 14340403d^{17} + 478961469d^{18} - 198558153d^{19} + 43610967d^{20} \\ & - 5364630d^{21} + 291600d^{22}. \end{aligned} \quad (3.6d)$$

The basis integrals themselves are in one-to-one correspondence with the diagrams. Unlike for the cut coefficients which factorize at each  $x_i$ , the integrals only properly factorize at  $x_i = 1$  and are otherwise honest multi-loop integrals whose internal topology is determined by  $\sigma$ . We will refer to the integral factors based on the bulk vertex structure that makes up their topology. For instance, the integral topology corresponding to eq. (3.2) is



$$\begin{array}{c} I^{mn} \blacksquare \\ \text{---} \\ E \bullet \\ \text{---} \\ I^{ij} \blacksquare \end{array} \Rightarrow \left( \int \frac{d^d \ell}{(2\pi)^d} \frac{1}{-\ell^2 + \omega^2} \right)^2 = \mathcal{I}_\emptyset^2 \quad (3.7)$$

and the one for  $\{2\}$  from eq. (3.3) is



$$\begin{array}{c} I^{mn} \blacksquare \\ \text{---} \\ E \bullet \\ \text{---} \\ E \bullet \\ \text{---} \\ I^{ij} \blacksquare \end{array} \Rightarrow \int \left( \prod_{i=1}^3 \frac{d^d \ell_i}{(2\pi)^d} \right) \frac{1}{(-\ell_1^2 + \omega^2)(-\ell_2^2 + \omega^2)(-\ell_3^2)(-(\ell_1 + \ell_2 + \ell_3)^2)} = \mathcal{I}_4. \quad (3.8)$$

We refer to the single-propagator integral that first appears in the radiation reaction as  $\mathcal{I}_\emptyset$ , and the next new topology (from  $\mathbb{T}^2$ ) that contains a 4-point vertex as  $\mathcal{I}_4$ . Luckily, many of the multi-loop integrals are relatively straightforward to evaluate, see appendix A.1, with the first difficult integral appearing at  $\mathbb{T}^4$ , see appendix A.2.

With both the coefficients and integrals, we can construct the effective action contribution as

$$S_{T^n} = \lambda_I^2 (\lambda_E \lambda_g)^n \int \frac{d\omega}{2\pi} \sum_{\sigma \in \mathfrak{S}_n} \frac{1}{|G_\sigma|} \left( \mathcal{R} \prod_{x_i \in \sigma} \mathcal{T}_{x_i} \right) \mathcal{I}_{G_\sigma}. \quad (3.9)$$

Applying the above construction algorithm does, of course, exactly reproduce the RR through  $T^4$  results of Ref. [20].

We note that the primary reason that this construction algorithm remains a conjecture is the integral basis decomposition. It is entirely possible that some higher-order tail will contain a necessary basis integral that is not captured via the integer partition scheme above. It would be interesting to see if modern integration methods like intersection theory [52, 53] would be able to shed light on this problem.

#### 4 Construction of tail-of-tail-of-tail-of-tail-of-tail ( $T^5$ )

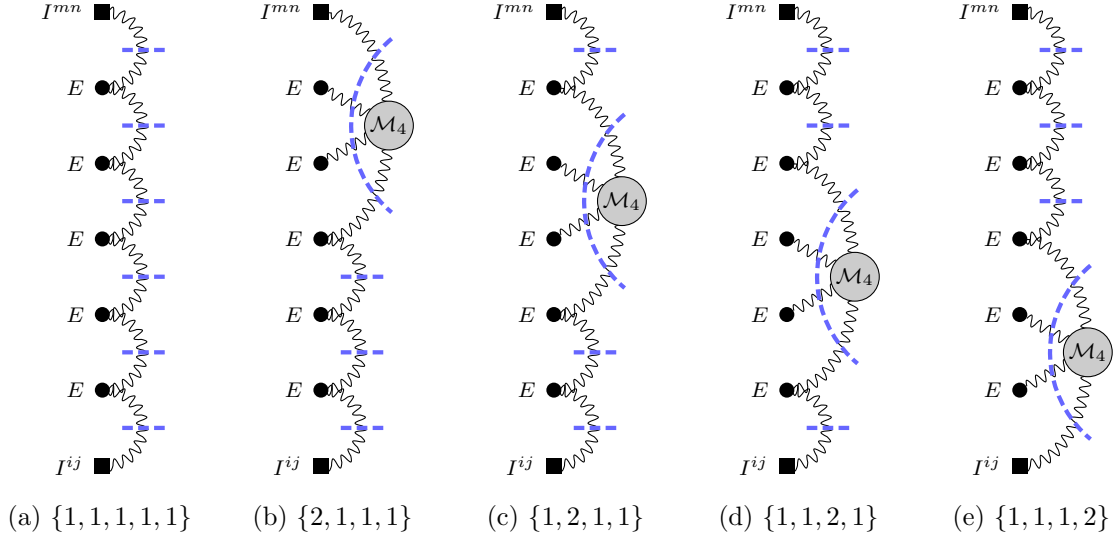


**Figure 1:** Diagrams for factorized contributions recycling data from radiation-reaction,  $T^1$ , and  $T^2$ , captioned by the permuted integer partition that generates them.

We now apply the tail construction algorithm to the case of  $T^5$ . First, we identify the nonequivalent permuted partitions of 5:

$$\mathfrak{s}_3 = \left\{ \begin{array}{cccc} \{1, 1, 1, 1, 1\} & \{3, 1, 1\} & \{4, 1\} & \{2, 3\} \\ \{2, 1, 1, 1\} & \{1, 3, 1\} & \{1, 4\} & \{3, 2\} \\ \{1, 2, 1, 1\} & \{1, 1, 3\} & \{1, 2, 2\} & \{2, 1, 2\} \\ \{1, 1, 2, 1\} & & \{2, 2, 1\} & \{5\} \\ \{1, 1, 1, 2\} & & & \end{array} \right\}. \quad (4.1)$$

From these partitions, we generate the actual diagrams. The first column is in fig. 1, the second in fig. 2, the third in fig. 3, and finally the fourth in fig. 4. The groupings are based on which tail order first produces the most complicated sub-topology.

The first three groups are all factorizing diagrams: they rely solely on data from previous loop orders as part of their computation. We start with the first group, fig. 1. There are two

distinct contributions in this group, fig. 1a and figs. 1b to 1e. The unitarity cut coefficients for these diagrams are simply

$$\overline{\text{Cut}}_{\{1,1,1,1,1\}} = \overline{\text{Cut}}_{\text{fig. 1a}} = \mathcal{R} \mathcal{T}_1^5 \quad (4.2)$$

$$\overline{\text{Cut}}_{\{2,1,1,1\}} = \overline{\text{Cut}}_{\text{fig. 1b}} = \overline{\text{Cut}}_{\text{fig. 1c}} = \overline{\text{Cut}}_{\text{fig. 1d}} = \overline{\text{Cut}}_{\text{fig. 1e}} = \mathcal{R} \mathcal{T}_1^3 \mathcal{T}_2 \quad (4.3)$$

with corresponding integrals and symmetry factors

$$\mathcal{I}_{\text{fig. 1a}} = \mathcal{I}_0^5 \quad (4.4)$$

$$|G_{\text{fig. 1a}}| = 2 \quad (4.5)$$

$$\mathcal{I}_{\text{fig. 1b}} = \mathcal{I}_{\text{fig. 1c}} = \mathcal{I}_{\text{fig. 1d}} = \mathcal{I}_{\text{fig. 1e}} = \mathcal{I}_4 \mathcal{I}_0^3 \quad (4.6)$$

$$|G_{\text{fig. 1b}}| = |G_{\text{fig. 1c}}| = |G_{\text{fig. 1d}}| = |G_{\text{fig. 1e}}| = 4. \quad (4.7)$$

As noted above, explicit expression for these integrals in terms of the dimensional regulator  $d$  are given in appendix A.1. The symmetry factors for figs. 1b to 1e stems from treating the potential modes and sources partaking in the bulk interaction as indistinguishable. The second set of diagrams, fig. 2, contains only diagrams which only have a single bulk  $\mathcal{M}_5$  graviton vertex. As such, all three have identical unitarity cut coefficients,

$$\overline{\text{Cut}}_{\{3,1,1\}} = \overline{\text{Cut}}_{\text{fig. 2a}} = \overline{\text{Cut}}_{\text{fig. 2b}} = \overline{\text{Cut}}_{\text{fig. 2c}} = \mathcal{R} \mathcal{T}_1^2 \mathcal{T}_3, \quad (4.8)$$

as well as basis integrals and symmetry factors

$$\mathcal{I}_{\text{fig. 2a}} = \mathcal{I}_{\text{fig. 2c}} = \mathcal{I}_{\text{fig. 2b}} = \mathcal{I}_5 \mathcal{I}_0^2 \quad (4.9)$$

$$|G_{\text{fig. 2a}}| = |G_{\text{fig. 2c}}| = |G_{\text{fig. 2b}}| = 2 \times 3! \quad (4.10)$$

The third group, shown in fig. 3, contains terms first seen in  $T^4$ . Their unitarity cut coefficients are easily computed as

$$\overline{\text{Cut}}_{\text{fig. 3a}} = \overline{\text{Cut}}_{\text{fig. 3b}} = \mathcal{R} \mathcal{T}_1 \mathcal{T}_4 \quad (4.11)$$

$$\overline{\text{Cut}}_{\text{fig. 3c}} = \overline{\text{Cut}}_{\text{fig. 3d}} = \mathcal{R} \mathcal{T}_1 \mathcal{T}_2^2. \quad (4.12)$$

The integrals and symmetry factors for figs. 3a and 3b are also straightforward to compute

$$\mathcal{I}_{\text{fig. 3a}} = \mathcal{I}_{\text{fig. 3b}} = \mathcal{I}_0 \mathcal{I}_6 \quad (4.13)$$

$$|G_{\text{fig. 3a}}| = |G_{\text{fig. 3b}}| = 2 \times 4!. \quad (4.14)$$

However, the integral-related contributions from figs. 3c and 3d,

$$\mathcal{I}_{\text{fig. 3c}} = \mathcal{I}_{\text{fig. 3d}} = \mathcal{I}_0 \mathcal{I}_{4 \otimes 4} \quad (4.15)$$

$$|G_{\text{fig. 3c}}| = |G_{\text{fig. 3d}}| = 2 \times 2 \times 2, \quad (4.16)$$

are more interesting because they mark the appearance of two different features of higher-order tails. First, these two diagrams share an integer partition – and thus unitarity coefficient

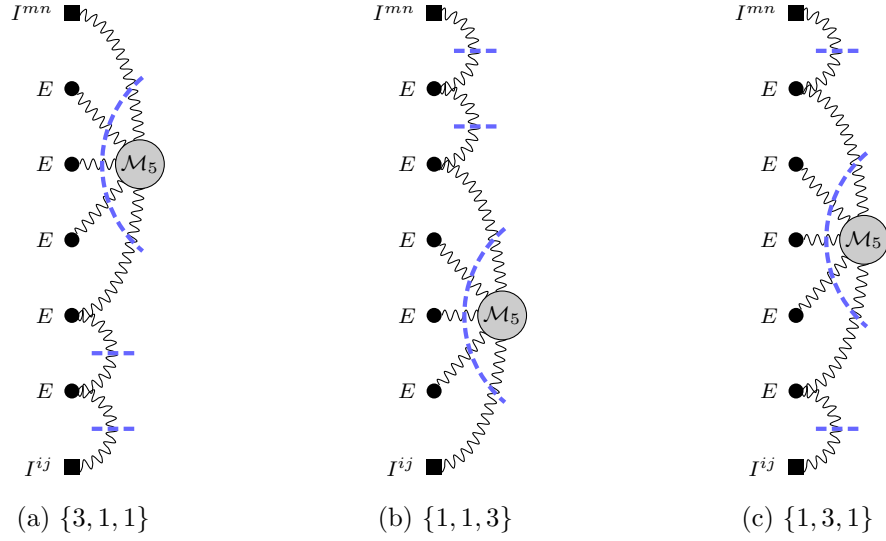


**Figure 2:** Diagrams that recycle the single  $\mathcal{M}_5$  bulk contribution first appearing at  $T^3$ , captioned by the permuted integer partition that generates them.

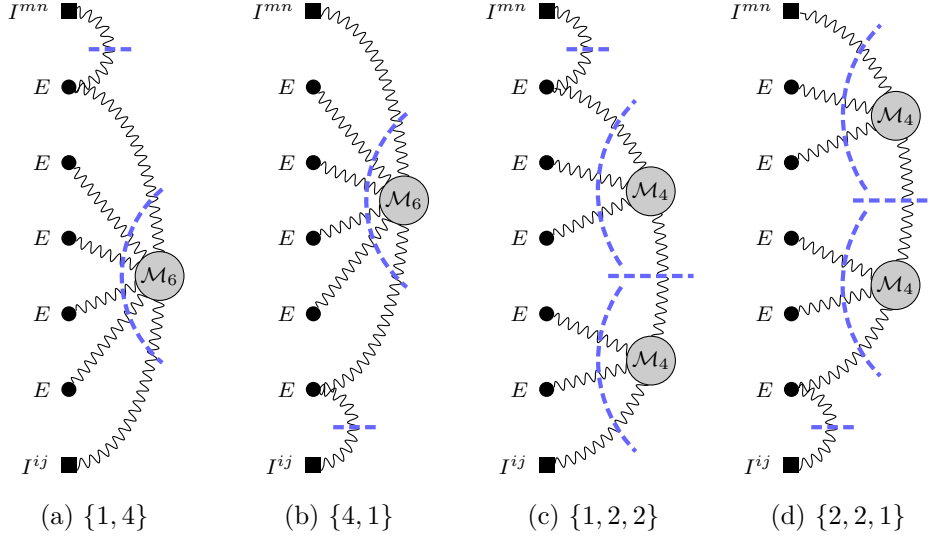


**Figure 3:** Diagrams whose factorization contains terms first appearing in  $T^4$ , captioned by the permuted integer partition that generates them.

– with fig. 4c, but differ at the level of their basis integrals. Second, the  $\mathcal{I}_{4 \otimes 4}$  integral that specifically appears in figs. 3c and 3d is nontrivial to evaluate in terms of generic functions of  $d$ . We instead rely on numerical evaluation, see appendix A.2.

We arrive at the final group, fig. 4. These are the diagrams which are in various senses “new” at  $T^5$ . Figures 4a and 4b follow naturally from the way that  $\{2, 2\}$  worked at  $T^4$ .

Their unitarity coefficients are given by

$$\overline{\text{Cut}}_{\text{fig. 4a}} = \overline{\text{Cut}}_{\text{fig. 4b}} = \mathcal{R} \mathcal{T}_2 \mathcal{T}_3 \quad (4.17)$$

with integrals and symmetries

$$\mathcal{I}_{\text{fig. 4a}} = \mathcal{I}_{\text{fig. 4b}} = \mathcal{I}_{4 \otimes 5} \quad (4.18)$$

$$|G_{\text{fig. 4a}}| = |G_{\text{fig. 4b}}| = 2 \times 2 \times 3!. \quad (4.19)$$

The novelty for these terms is the  $\mathcal{I}_{4 \otimes 5}$  which we again turn to numerical methods to evaluate, see appendix A.3. Next, fig. 4d, whose interest we alluded to above. This diagram is the first case of two non-trivial topologies joining at a source contact, and thus the first instance of the order of the permuted integer partition actually mattering. As figs. 3c and 3d above, the unitarity coefficient is given by

$$\overline{\text{Cut}}_{\text{fig. 4c}} = \mathcal{R} \mathcal{T}_1 \mathcal{T}_2^2 \quad (4.20)$$

but the integral for this diagram actually factorizes,

$$\mathcal{I}_{\text{fig. 4c}} = \mathcal{I}_4^2 \quad (4.21)$$

$$|G_{\text{fig. 4c}}| = 2 \times 2 \times 2, \quad (4.22)$$

unlike the other two. In fact, understanding this distinction between fig. 4c and figs. 3c and 3d was key to arriving at eqs. (3.4) and (3.9).

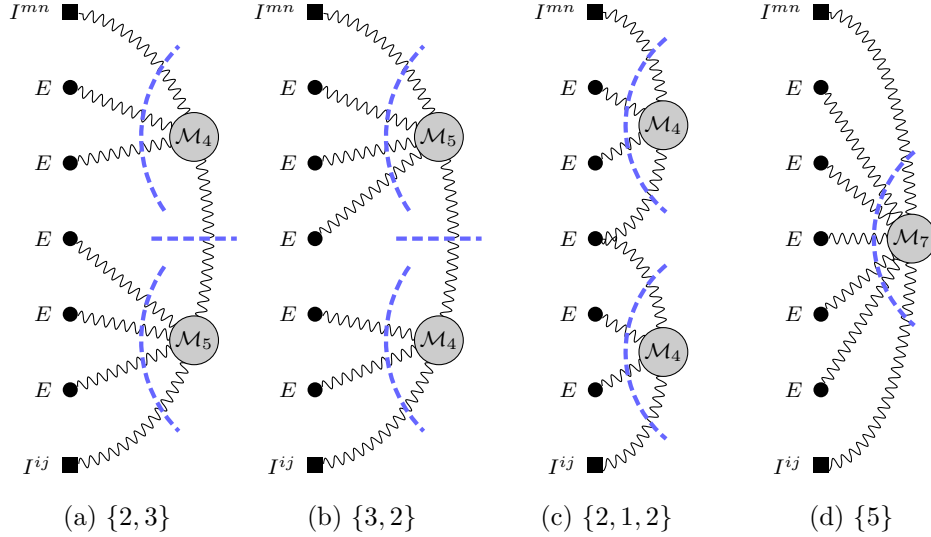


**Figure 4:** Diagrams newly appearing at  $T^5$ , captioned by the permuted integer partition that generates them.

Last, but certainly not least, we arrive at the one diagram that cannot be computed from lower-loop data, fig. 4d. The basis integral and symmetry factor for this diagram are simple

enough,

$$\mathcal{I}_{\text{fig. 4d}} = \mathcal{I}_7 \quad (4.23)$$

$$|G_{\text{fig. 4d}}| = 2 \times 5!, \quad (4.24)$$

but the unitarity coefficient must be newly computed. To do so, we need to compute

$$\text{Cut}_{\text{fig. 4d}} = \lambda_I^2 J^{\mu\nu} J^{\rho\sigma} \left( \prod_{i=1}^5 \mathcal{M}_{Eg}^{\alpha_i\beta_i} P^{\alpha_i\beta_i;\gamma_i\delta_i} \right) P^{\mu\nu;\gamma_0\delta_0} P^{\rho\sigma;\gamma_6\delta_6} \mathcal{M}_{g^7}^{\gamma_0\delta_0\dots\gamma_6\delta_6} \quad (4.25)$$

using eqs. (2.9), (2.11), (2.12) and (2.14). The numerator for the tree amplitude has hundreds of thousands of terms, which is further dressed with 7200 distinct combinations of relabelings and propagators. As such, it was vitally important to employ both the tensor reduction method of Ref. [20] and the state sewing method of Ref. [54] to reduce the proliferation of extraneous terms. After constructing the loop-momentum-dependent unitarity cut, we need to reduce it to the integral basis using integration by parts relations. We employ a lightly-modified version of FIRE 6.5 [55] to enact the integral reduction, and then extract the coefficient of the  $\mathcal{I}_7$  basis integral. This step in the process also provides a cross-check of the proposed integral basis: in general we expect the reduction of this diagram *without cut conditions* to produce terms for every element of the integral basis, providing an opportunity to identify any missing integrals. However, the only term which will be correct is the one whose final propagator structure matches the cut topology,  $\mathcal{T}_5 \mathcal{I}_7$ . Additionally, the figs. 4a and 4b topologies are factorization channels of fig. 4d, and thus the reduction of  $\text{Cut}_{\text{fig. 4d}}$  will actually produce the correct coefficients for them as well, up to relative symmetry factors. At the conclusion of this process, we find the cut coefficient

$$\overline{\text{Cut}}_{\text{fig. 4d}} = \frac{\mathcal{R} \mathcal{P}_{25}}{6\mathcal{D}_3^4 \mathcal{D}_1 (d-2)d(2d-3)(3d-5)(5d-6)(5d-8)(3d-2)^2(3d-4)^2} \quad (4.26)$$

with numerator polynomial

$$\begin{aligned} \mathcal{P}_{25} = & 570621542400 - 3817851770880d + 10461421320192d^2 \\ & - 15448588835328d^3 + 14470772087808d^4 - 11533634757504d^5 \\ & + 10359103552000d^6 - 8174350894336d^7 + 3835795527664d^8 \\ & - 412015363192d^9 - 640904151652d^{10} + 441788353428d^{11} \\ & - 49414187298d^{12} - 213527363567d^{13} + 340041180553d^{14} \\ & - 370751638979d^{15} + 309491168905d^{16} - 190018152600d^{17} \\ & + 83761403414d^{18} - 26470493490d^{19} + 6063243616d^{20} \\ & - 1017098367d^{21} + 119676213d^{22} - 7235055d^{23} - 289575d^{24} \\ & + 60750d^{25}. \end{aligned} \quad (4.27)$$

Finally, we can combine all of the contributions using eq. (3.9), evaluate all of the integrals using appendix A, and series expand in the dimension regularization parameter  $d \rightarrow 3 - 2\epsilon$  to arrive at<sup>1</sup>

$$\begin{aligned}
S_{T^5} = & -\frac{1}{5} \frac{107^2}{105^2} G_N^6 E^5 \int \frac{d\omega}{2\pi} \omega^{10} \kappa_{-+}(\omega) \left\{ \frac{1}{6\epsilon^3} + \frac{1}{\epsilon^2} \left[ \frac{3709423}{686940} - \log \left( \frac{\omega^2 e^{\gamma_E}}{\mu^2 \pi} \right) + i\pi \operatorname{sgn}(\omega) \right] \right. \\
& + \frac{1}{\epsilon} \left[ \frac{305250541109}{3029405400} - \frac{49}{2} \zeta_2 - \frac{1680}{107} \zeta_3 + 3 \log \left( \frac{\omega^2 e^{\gamma_E}}{\mu^2 \pi} \right)^2 - \frac{3709423}{114490} \log \left( \frac{\omega^2 e^{\gamma_E}}{\mu^2 \pi} \right) \right. \\
& \left. \left. + i\pi \operatorname{sgn}(\omega) \left( \frac{3709423}{114490} - 6 \log \left( \frac{\omega^2 e^{\gamma_E}}{\mu^2 \pi} \right) \right) \right] \right. \\
& + \left[ \text{Real and } \omega\text{-even terms dependent on } \mathcal{I}_{4 \otimes 4} \Big|_{\epsilon^3} \right. \\
& \left. + i\pi \operatorname{sgn}(\omega) \left( \frac{305250541109}{504900900} - 75 \zeta_2 - \frac{10080}{107} \zeta_3 - \frac{11128269}{57245} \log \left( \frac{\omega^2 e^{\gamma_E}}{\mu^2 \pi} \right) \right. \right. \\
& \left. \left. + 18 \log \left( \frac{\omega^2 e^{\gamma_E}}{\mu^2 \pi} \right)^2 \right) \right] \\
& \left. + \mathcal{O}(\epsilon) \right\}, \tag{4.28}
\end{aligned}$$

where  $\zeta_i$  is the Riemann zeta values,  $\gamma_E$  is Euler's gamma constant, and  $\mu$  is the renormalization scale associated to dimensional regularization. Notably, every single individual cut's contribution to the effective action begins at  $\mathcal{O}(\epsilon^5)$ . It is highly nontrivial, and a mark of internal consistency, that both the leading and subleading divergences cancel between all of the contributions.

## 5 Radiated energy and renormalization of the quadrupole coupling

We employ the CTP energy extraction method, explained in Refs. [20, 34, 37–39], to the  $T^5$  CTP effective action, eq. (4.28). Within the framework of quadrupole tails, the process amounts to extracting the  $\omega$ -odd part of the effective action integrand, eq. (2.6), and then multiplying the resulting term by  $(-i\omega)$

$$\Delta E = \int d\omega \left[ (-i\omega) f_{\text{odd}}(\omega) \underbrace{I^{ij}(\omega) I_{ij}(-\omega)}_{\kappa(\omega)} \right]. \tag{5.1}$$

In the current case of  $T^5$  (as well as all previous odd-order tails [19, 20, 36]), the CTP energy extraction is exactly equivalent to simply taking the coefficient of  $i \operatorname{sgn}(\omega)$  in the integrand, multiplying it by  $\omega$ , and then sending  $\kappa_{-+}(\omega) \rightarrow 2\kappa(\omega)$  (where  $\kappa(\omega)$  is the contraction of the

---

<sup>1</sup>Note that this is a different dimensional regularization scheme choice than Ref. [20], which uses  $d \rightarrow 3 + \epsilon$ . Such differences will drop out of the final observables.

physical quadrupoles). Following through this process, we arrive at

$$\begin{aligned}
(\Delta E)_{\text{T}^5} = & -\frac{1}{5} \frac{107^2}{105^2} G_N^6 E^5 \int_{-\infty}^{\infty} d\omega \kappa(\omega) \omega^{11} \left\{ \frac{1}{\epsilon^2} + \frac{1}{\epsilon} \left[ \frac{3709423}{114490} - 6 \log \left( \frac{\omega^2 e^{\gamma_E}}{\mu^2 \pi} \right) \right] \right. \\
& + \left[ \frac{305250541109}{504900900} - 75 \zeta_2 - \frac{10080}{107} \zeta_3 \right. \\
& \left. \left. - \frac{11128269}{57245} \log \left( \frac{\omega^2 e^{\gamma_E}}{\mu^2 \pi} \right) + 18 \log \left( \frac{\omega^2 e^{\gamma_E}}{\mu^2 \pi} \right)^2 \right] + \mathcal{O}(\epsilon^1) \right\}. \quad (5.2)
\end{aligned}$$

We next need to construct the  $\mathcal{O}(G_N^6)$ -inclusive energy dissipation and remove the dimensional regularization poles by renormalizing the quadrupole coupling.

The first step of this process is to lift the quadrupole coupling to a function of  $\epsilon$  and the other parameters of the problem. In a slight abuse of notation, we will attach this coupling modification to  $\kappa(\omega)$  rather than  $\lambda_I$ :

$$\kappa(\omega) \rightarrow \kappa'(\omega) \equiv \kappa(\omega, \mu) Z(d, \omega, G_N, E). \quad (5.3)$$

$Z(d, \omega, G_N, E)$  is a polynomial in  $\omega$ ,  $G_N$ ,  $E$ , and  $(d-3)^{-1}$  whose coefficients are fixed by demanding that the physical observable is free of dimensional regulator divergences. Note that we have also introduced a  $\mu$ -dependence to  $\kappa$ , which will be relevant for studying the renormalization group flow below. Ref. [20] identified  $Z(d, \omega, G_N, E)$  through  $\mathcal{O}(G_N^4)$  as<sup>2</sup>

$$\begin{aligned}
\kappa'(\omega) \equiv \kappa(\omega, \mu) & \left( 1 + 2 \frac{107}{105} \frac{(G_N E \omega)^2}{(d-3)} \left( 1 + \frac{107}{105} \frac{(G_N E \omega)^2}{(d-3)} \right) \right. \\
& \left. + \frac{1695233}{105^3} \frac{(G_N E \omega)^4}{(d-3)} + \mathcal{O}(G_N^5) \right). \quad (5.4)
\end{aligned}$$

In principle, there could be a new contribution at  $\mathcal{O}(G_N^5)$  which would only be detectable via the new  $\text{T}^5$  terms. Assembling the total energy dissipation of the tails, including the leading order radiation-reaction term  $(\Delta E)_{\text{RR}}$ , via

$$\overline{(\Delta E)}_{\text{T}^5} = [(\Delta E)_{\text{RR}} + (\Delta E)_{\text{T}} + (\Delta E)_{\text{T}^2} + (\Delta E)_{\text{T}^3} + (\Delta E)_{\text{T}^4} + (\Delta E)_{\text{T}^5}] \Big|_{\kappa \rightarrow \kappa'} \quad (5.5)$$

we find that all of the divergences cancel through  $\mathcal{O}(G_N^6)$  without needing to introduce a  $\mathcal{O}(G_N^5)$  correction. The leading  $\mathcal{O}(\epsilon^{-2})$  divergence cancels against  $(\Delta E)_{\text{T}}$  augmented by the  $\frac{G_N^4}{(d-3)^2}$  from eq. (5.4). The cancellation of the subleading divergence results from a more-complicated interplay between  $(\Delta E)_{\text{T}}$  and  $(\Delta E)_{\text{T}^3}$  and the remaining terms of eq. (5.4).

---

<sup>2</sup>Note that Ref. [20] used the dimensional regularization scheme  $d \rightarrow 3 + \epsilon$ , which we have lifted to a scheme-agnostic statement here.



Having dealt with the divergences, we find the physical energy loss through  $G_N^6$  to be

$$\begin{aligned}
(\overline{\Delta E})_{T^5} = (\overline{\Delta E})_{T^4} + G_N^6 E^5 \frac{2}{5} \frac{107^2}{105^2} \int_{-\infty}^{\infty} d\omega \kappa(\omega, \mu) \omega^{11} & \left[ -\frac{1379886245}{10098018} + \frac{1680}{107} \zeta_3 + 12\zeta_2 \right. \\
& \left. - 2 \log \left( \frac{\omega^2 e^{\gamma_E}}{\mu^2 \pi} \right)^2 + \frac{24905541}{801430} \log \left( \frac{\omega^2 e^{\gamma_E}}{\mu^2 \pi} \right) \right] \quad (5.6)
\end{aligned}$$

where  $(\overline{\Delta E})_{T^4}$  was derived in Ref. [20].

Finally, we look at the RG flow of the now  $\mu$ -dependent  $\kappa$ . As an observable, the energy loss must be independent of the reference energy scale  $\mu$ . Thus, the  $T^5$  energy loss must obey

$$\frac{d}{d\mu} (\overline{\Delta E})_{T^5} = 0 + \mathcal{O}(G_N^7), \quad (5.7)$$

generating a classical renormalization group flow. Since there was no new contribution to the renormalized source coupling due to  $T^5$ , we should also suspect there to be no  $\mathcal{O}(G_N^5)$  contribution to the RG flow of  $\kappa(\omega, \mu)$ . Indeed, we find that eq. (5.7) leads to an RG equation for  $\kappa(\omega, \mu)$

$$\frac{d}{d \log \mu} \kappa(\omega, \mu) = -(2G_N E \omega)^2 \kappa(\omega, \mu) \left( \frac{107}{105} + \frac{1695233}{105^3} (G_N E \omega)^2 \right) + \mathcal{O}(G_N^6) \quad (5.8)$$

in exact agreement with Ref. [20], but additionally establishing the lack of  $G_N^5$  corrections.

## 6 Conclusion

This work proposed a tail construction algorithm based on permuted integer partitions, eq. (3.9), and applied it to the computation of  $T^5$ . This necessitated computing a novel generalized unitarity basis coefficient, eq. (4.26). The new effective action contribution, eq. (4.28), led to a corresponding correction to the gravitational wave energy flux, eq. (5.6).

The permuted integer partition algorithm developed here exploits the organization of the problem using generalized unitarity methods to systematically recycle lower-loop data and identify the minimal *new* data needed at each loop order. Should the algorithm continue to hold at higher loops, it predicts that there is exactly one new integral coefficient needed at each loop order. The novel 6-loop coefficient was computed via sewing a seven-point bulk graviton amplitude to the relevant source-analogous amplitudes, as seen in fig. 4d.

Combining the new coefficient with the iteration terms produced the 6-loop contribution to the tail effective action. This effective action encodes, among other dynamics, the energy loss of the quadrupole into the gravitational field, which by energy balance is opposite to the energy radiated in the form of gravitational waves. Notably, the new contribution coming from  $T^5$ , eq. (5.6), is *simpler* (in terms of  $\zeta$  values which appear) than the  $T^4$  contribution found in Ref. [20] – a similar but less-stark difference exists between  $T^2$  and  $T^3$ . The new radiated energy contribution leads to a renormalization group flow of the quadrupole coupling, eq. (5.2), in exact agreement with the RG equation found in Ref. [20].

From a theoretical standpoint, it would be interesting to proceed to the next order,  $T^6$ , both to verify the continued validity of the proposed construction algorithm, and also because there will almost certainly be new contributions to the renormalization and RG flow of the quadrupole coupling, eqs. (5.4) and (5.8). However, it seems difficult that this step could be achieved simply by repeating the cut sewing and reduction used here, as it suffers from worse-than-factorial growth in many stages of the computation. A particularly useful bypass of this problem would be understanding the relationships between the  $\mathcal{T}_i$  in order to find a method of constructing them directly. A tantalizing hint in this direction is that the irreducible polynomials appearing in the numerators of eqs. (3.5b) to (3.5e) and (4.26) double in degree when going from odd to even order, but only increase their degree by 3 when going from even to odd.

There are also a number of interesting followup directions that do not necessitate knowing  $\mathcal{T}_6$ . For instance, eq. (3.9) provides a route to resumming various sub-classes of terms whose constituent  $\mathcal{T}_i$  and  $\mathcal{I}_G$  are already known. Analyzing such terms and comparing them with other resummation schemes, e.g. eikonal, could prove enlightening. Additionally, it would be worthwhile to examine how the more subtle memory effects [56–64] can be captured using these types of generalized unitarity methods. Finally, since this framework for computing tails only relies on the validity of the multipole expansion of the stress-energy tensor – with no explicit reference to a binary system – it would be worthwhile to explore the connection with other methods for studying compact gravitating objects, like black hole perturbation theory or deformations of neutron stars.

## Acknowledgments

I would like to thank Michèle Levi, Julio Parra-Martinez, Nic Pavao, Fei Teng, Radu Roiban, and John Joseph Carrasco for discussion on this and related projects. I am grateful to Sasank Chava, Julio Parra-Martinez, Nic Pavao, and Radu Roiban for feedback on the manuscript. I would also like to thank Alexander Smirnov for providing guidance on modifying FIRE to accommodate this work’s integral reduction problem.

This research was supported by the US DOE under contract DE-SC0015910 and by Northwestern University via the Amplitudes and Insight Group, Department of Physics and Astronomy, and Weinberg College of Arts and Sciences. This research would not have been possible without the computational resources and staff contributions provided for the Quest high performance computing facility at Northwestern University which is jointly supported by the Office of the Provost, the Office for Research, and Northwestern University Information Technology.

fillT<sub>E</sub>X was used as part of writing the bibliography [65].

## A Integrals

Due to the factorization of the basis integrals, all but two of the needed integral evaluations ( $\mathcal{I}_{4\otimes 5}$  and  $\mathcal{I}_7$ ) can be recycled from lower loop orders.  $\mathcal{I}_{4\otimes 5}$  requires numerical evaluation, and is discussed below in appendix A.3.  $\mathcal{I}_7$  can be evaluated using “bubble iteration” in terms of ratios of  $\Gamma$ -functions, similar to previous loop orders.

### A.1 Analytic evaluations

Here we state without derivation the analytic expressions needed for the basis integrals corresponding to figs. 1, 2, 3a, 3b, 4c and 4d, i.e. eqs. (4.4), (4.6) and (4.9). Interested readers can find a more complete discussion in Ref. [20], which primarily relies on the integrals tables from Ref. [66].

First, the ratios of  $\Gamma$ -functions that appear in the recursive evaluation of the integrals

$$A_{\lambda_1, \lambda_2; d} = \frac{\Gamma(d/2 - \lambda_1)\Gamma(d/2 - \lambda_2)\Gamma(\lambda_1 + \lambda_2 - d/2)}{\Gamma(\lambda_1)\Gamma(\lambda_2)\Gamma(d - \lambda_1 - \lambda_2)}, \quad (\text{A.1})$$

$$B_{\lambda_1, \lambda_2, \lambda_3; d} = \frac{\Gamma(\lambda_1 + \lambda_3 - d/2)\Gamma(\lambda_2 + \lambda_3 - d/2)\Gamma(d/2 - \lambda_3)\Gamma(\lambda_1 + \lambda_2 + \lambda_3 - d)}{\Gamma(\lambda_1)\Gamma(\lambda_2)\Gamma(\lambda_1 + \lambda_2 + 2\lambda_3 - d)}. \quad (\text{A.2})$$

Then the needed integrals

$$\mathcal{I}_\emptyset = (-1)(4\pi)^{-d/2}(-\omega^2)^{d/2-1}, \quad (\text{A.3})$$

$$\mathcal{I}_4 = (4\pi)^{-3d/2} A_{1,1;d} B_{1,1,2-d/2;d} (-\omega^2)^{3d/2-4}, \quad (\text{A.4})$$

$$\mathcal{I}_5 = (4\pi)^{-2d} A_{1,1;d} A_{1,2-d/2;d} B_{1,1,3-d;d} (-\omega^2)^{2d-5}, \quad (\text{A.5})$$

$$\mathcal{I}_6 = (4\pi)^{-5d/2} A_{1,1;d} A_{1,2-d/2;d} A_{1,3-d;d} B_{1,1,4-3d/2;d} (-\omega^2)^{5d/2-6}, \quad (\text{A.6})$$

$$\mathcal{I}_7 = (4\pi)^{-3d} A_{1,1;d} A_{1,2-d/2;d} A_{1,3-d;d} A_{1,4-3d/2;d} B_{1,1,5-2d;d} (-\omega^2)^{3d-7}. \quad (\text{A.7})$$

### A.2 Numeric evaluation of figs. 3c and 3d

The integrals for figs. 3c and 3d factorize into a tadpole integral and an integral that we refer to as  $\mathcal{I}_{4\otimes 4}$ . This integral is currently unknown analytically, but was numerically evaluated [67] and reconstructed into known transcendental numbers [68, 69] in Ref. [20]. We reproduce the integral here for completeness. First, we note that the  $\omega$  dependence of the integral can be factorized

$$\mathcal{I}_{4\otimes 4} = (-\omega^2)^{5d/2-7} \mathcal{I}_{4\otimes 4}(1). \quad (\text{A.8})$$

We find that the remaining integral evaluates to

$$\begin{aligned}
\mathcal{I}_{4\otimes 4}(1) = \frac{1}{8(4\pi)^5} & \left[ \frac{1}{\epsilon^2} + \frac{16 + 5(\log(\pi) - \gamma_E)}{\epsilon} \right. \\
& + \left( 184 + \frac{47}{2}\zeta_2 + 80(\log(\pi) - \gamma_E) + \frac{25}{2}(\log(\pi) - \gamma_E)^2 \right) \\
& + \epsilon \left( 1888 + 408\zeta_2 - \frac{611}{3}\zeta_3 + (\log(\pi) - \gamma_E) \left( 920 + \frac{235}{2}\zeta_2 \right) \right. \\
& \quad \left. + 200(\log(\pi) - \gamma_E)^2 + \frac{125}{6}(\log(\pi) - \gamma_E)^3 \right) \\
& \epsilon^2 \left( 18544 + 5092\zeta_2 - \frac{9872}{3}\zeta_3 + \frac{42193}{40}\zeta_2^2 \right. \\
& \quad + (\log(\pi) - \gamma_E) \left( 9440 + 2040\zeta_2 - \frac{3055}{3}\zeta_3 \right) \\
& \quad + (\log(\pi) - \gamma_E)^2 \left( 2300 + \frac{1175}{4}\zeta_2 \right) \\
& \quad + \frac{1000}{3}(\log(\pi) - \gamma_E)^3 + \frac{625}{24}(\log(\pi) - \gamma_E)^4 \Big) \\
& \left. + 255097.168799191 \epsilon^3 + \mathcal{O}(\epsilon^4) \right]. \tag{A.9}
\end{aligned}$$

Note the finite precision coefficient of  $\epsilon^3$ . We do not yet have a transcendental representation for this term. Is this relevant to the radiated energy computed above? In the computation of eq. (4.28), we tagged this term and found that it contributes to the *conservative* piece of the effective action, but not the *dissipative* piece that we analyze in this paper.

### A.3 Numeric evaluation of figs. 4a and 4b

The integral needed for figs. 4a and 4b, which we will refer to as  $\mathcal{I}_{4\otimes 5}$ , are similar to  $\mathcal{I}_{4\otimes 4}$ . If we knew an analytic form of  $\mathcal{I}_{4\otimes 4}$ , we could use “bubble iteration” to recursively evaluate both in terms of the same base functions. Unfortunately, we instead need to perform a numerical evaluation and PSLQ reconstruction [68] of  $\mathcal{I}_{4\otimes 5}$  as well. As above, we will factorize the  $\omega$ -dependence out of the integral for the numerical evaluation

$$\mathcal{I}_{4\otimes 5} = (-\omega^2)^{3d-8} \mathcal{I}_{4\otimes 5}(1). \tag{A.10}$$

We use AMFlow [67] connected to Kira [70] for the numerical evaluation. After reconstruction, we find

$$\begin{aligned}
\mathcal{I}_{4\otimes 5}(1) = & \frac{1}{96(4\pi)^6} \left[ \frac{11}{\epsilon^2} + \frac{1}{\epsilon} \left( 208 + 66(\log(\pi) - \gamma_E) \right) \right. \\
& + 3(856 + 113\zeta_2 + 416(\log(\pi) - \gamma_E) + 66(\log(\pi) - \gamma_E)^2) \\
& + \epsilon \left( 26528 + 6672\zeta_2 - 1658\zeta_3 + (\log(\pi) - \gamma_E)(15408 + 2034\zeta_2) \right. \\
& \quad \left. + 3744(\log(\pi) - \gamma_E)^2 + 396(\log(\pi) - \gamma_E)^3 \right) \\
& \epsilon^2 \left( 251344 + 86472\zeta_2 - 33184\zeta_3 + \frac{96837}{4}\zeta_4 \right. \\
& \quad + (\log(\pi) - \gamma_E)(159168 + 40032\zeta_2 - 9948\zeta_3) \\
& \quad + (\log(\pi) - \gamma_E)^2(46224 + 6102\zeta_2) \\
& \quad \left. + 7488(\log(\pi) - \gamma_E)^3 + 594(\log(\pi) - \gamma_E)^4 \right) \\
& + \epsilon^3 \left( 2288256 + 945312\zeta_2 - 438384\zeta_3 + 502284\zeta_4 - \frac{349086}{5}\zeta_5 - 60522\zeta_2\zeta_3 \right. \\
& \quad + (\log(\pi) - \gamma_E)(1508064 + 518832\zeta_2 - 199104\zeta_3 + \frac{290511}{2}\zeta_4) \\
& \quad + (\log(\pi) - \gamma_E)^2(477504 + 120096\zeta_2 - 29844\zeta_3) \\
& \quad + (\log(\pi) - \gamma_E)^3(92448 + 12204\zeta_2) + 11232(\log(\pi) - \gamma_E)^4 \\
& \quad \left. + \frac{3564}{5}(\log(\pi) - \gamma_E)^5 \right) + \mathcal{O}(\epsilon^4) \Big] \tag{A.11}
\end{aligned}$$

Given that the unitarity coefficient of this integral, eq. (4.17), contains an  $\epsilon^{-3}$  pole, we only require the value of  $\mathcal{I}_{4\otimes 5}(1)$  through the stated  $\mathcal{O}(\epsilon^3)$  in order to extract the finite contribution to the effective action and energy loss.

## References

- [1] LIGO SCIENTIFIC collaboration, J. Aasi et al., *Advanced LIGO*, *Class. Quant. Grav.* **32** (2015) 074001 [[1411.4547](#)].
- [2] VIRGO collaboration, F. Acernese et al., *Advanced Virgo: a second-generation interferometric gravitational wave detector*, *Class. Quant. Grav.* **32** (2015) 024001 [[1408.3978](#)].
- [3] KAGRA collaboration, T. Akutsu et al., *Overview of KAGRA: Detector design and construction history*, *PTEP* **2021** (2021) 05A101 [[2005.05574](#)].
- [4] T. Damour, P. Jaranowski and G. Schäfer, *Nonlocal-in-time action for the fourth post-Newtonian conservative dynamics of two-body systems*, *Phys. Rev. D* **89** (2014) 064058 [[1401.4548](#)].

- [5] L. Blanchet, *Gravitational Radiation from Post-Newtonian Sources and Inspiralling Compact Binaries*, *Living Rev. Rel.* **17** (2014) 2 [[1310.1528](#)].
- [6] L. Blanchet, *Post-Newtonian theory for gravitational waves*, *Living Rev. Rel.* **27** (2024) 4.
- [7] W. D. Goldberger and I. Z. Rothstein, *An Effective field theory of gravity for extended objects*, *Phys. Rev. D* **73** (2006) 104029 [[hep-th/0409156](#)].
- [8] B. Kol and M. Smolkin, *Classical Effective Field Theory and Caged Black Holes*, *Phys. Rev.* **D77** (2008) 064033 [[0712.2822](#)].
- [9] B. Kol and M. Smolkin, *Non-Relativistic Gravitation: From Newton to Einstein and Back*, *Class. Quant. Grav.* **25** (2008) 145011 [[0712.4116](#)].
- [10] B. Kol and M. Smolkin, *Dressing the Post-Newtonian two-body problem and Classical Effective Field Theory*, *Phys. Rev. D* **80** (2009) 124044 [[0910.5222](#)].
- [11] B. Kol, M. Levi and M. Smolkin, *Comparing space+time decompositions in the post-Newtonian limit*, *Class. Quant. Grav.* **28** (2011) 145021 [[1011.6024](#)].
- [12] L. Bernard, L. Blanchet, A. Bohé, G. Faye and S. Marsat, *Fokker action of nonspinning compact binaries at the fourth post-Newtonian approximation*, *Phys. Rev.* **D93** (2016) 084037 [[1512.02876](#)].
- [13] L. Blanchet and T. Damour, *Hereditary effects in gravitational radiation*, *Phys. Rev. D* **46** (1992) 4304.
- [14] L. Blanchet and T. Damour, *Tail Transported Temporal Correlations in the Dynamics of a Gravitating System*, *Phys. Rev. D* **37** (1988) 1410.
- [15] G. Kälin and R. A. Porto, *From Boundary Data to Bound States*, *JHEP* **01** (2020) 072 [[1910.03008](#)].
- [16] G. Kälin and R. A. Porto, *From boundary data to bound states. Part II. Scattering angle to dynamical invariants (with twist)*, *JHEP* **02** (2020) 120 [[1911.09130](#)].
- [17] G. Cho, G. Kälin and R. A. Porto, *From boundary data to bound states. Part III. Radiative effects*, *JHEP* **04** (2022) 154 [[2112.03976](#)].
- [18] A. Buonanno, M. Khalil, D. O’Connell, R. Roiban, M. P. Solon and M. Zeng, *Snowmass White Paper: Gravitational Waves and Scattering Amplitudes*, in *Snowmass 2021*, 4, 2022, [2204.05194](#).
- [19] A. Edison and M. Levi, *A tale of tails through generalized unitarity*, *Phys. Lett. B* **837** (2023) 137634 [[2202.04674](#)].
- [20] A. Edison and M. Levi, *Higher-order tails and RG flows due to scattering of gravitational radiation from binary inspirals*, *JHEP* **08** (2024) 161 [[2310.20066](#)].
- [21] T. Marchand, L. Blanchet and G. Faye, *Gravitational-wave tail effects to quartic non-linear order*, *Class. Quant. Grav.* **33** (2016) 244003 [[1607.07601](#)].
- [22] R. Fujita, *Gravitational radiation for extreme mass ratio inspirals to the 14th post-Newtonian order*, *Prog. Theor. Phys.* **127** (2012) 583 [[1104.5615](#)].
- [23] R. Fujita, *Gravitational Waves from a Particle in Circular Orbits around a Schwarzschild Black Hole to the 22nd Post-Newtonian Order*, *Prog. Theor. Phys.* **128** (2012) 971 [[1211.5535](#)].

- [24] L. Barack and A. Pound, *Self-force and radiation reaction in general relativity*, *Rept. Prog. Phys.* **82** (2019) 016904 [[1805.10385](#)].
- [25] N. Warburton, A. Pound, B. Wardell, J. Miller and L. Durkan, *Gravitational-Wave Energy Flux for Compact Binaries through Second Order in the Mass Ratio*, *Phys. Rev. Lett.* **127** (2021) 151102 [[2107.01298](#)].
- [26] M. Levi, *Effective Field Theories of Post-Newtonian Gravity: A comprehensive review*, *Rept. Prog. Phys.* **83** (2020) 075901 [[1807.01699](#)].
- [27] R. A. Porto, *The effective field theorist's approach to gravitational dynamics*, *Phys. Rept.* **633** (2016) 1 [[1601.04914](#)].
- [28] W. D. Goldberger and A. Ross, *Gravitational radiative corrections from effective field theory*, *Phys. Rev. D* **81** (2010) 124015 [[0912.4254](#)].
- [29] M. Levi, *Next to Leading Order gravitational Spin-Orbit coupling in an Effective Field Theory approach*, *Phys. Rev. D* **82** (2010) 104004 [[1006.4139](#)].
- [30] A. Ross, *Multipole expansion at the level of the action*, *Phys. Rev. D* **85** (2012) 125033 [[1202.4750](#)].
- [31] M. Levi and J. Steinhoff, *Spinning gravitating objects in the effective field theory in the post-Newtonian scheme*, *JHEP* **09** (2015) 219 [[1501.04956](#)].
- [32] Q. Henry and F. Larrouturou, *Conservative tail and failed-tail effects at the fifth post-Newtonian order*, *Phys. Rev. D* **108** (2023) 084048 [[2307.05860](#)].
- [33] G. L. Almeida, S. Foffa and R. Sturani, *Gravitational multipole renormalization*, *Phys. Rev. D* **104** (2021) 084095 [[2107.02634](#)].
- [34] C. R. Galley and M. Tiglio, *Radiation reaction and gravitational waves in the effective field theory approach*, *Phys. Rev. D* **79** (2009) 124027 [[0903.1122](#)].
- [35] S. Foffa and R. Sturani, *Tail terms in gravitational radiation reaction via effective field theory*, *Phys. Rev. D* **87** (2013) 044056 [[1111.5488](#)].
- [36] C. R. Galley, A. K. Leibovich, R. A. Porto and A. Ross, *Tail effect in gravitational radiation reaction: Time nonlocality and renormalization group evolution*, *Phys. Rev. D* **93** (2016) 124010 [[1511.07379](#)].
- [37] C. R. Galley and A. K. Leibovich, *Radiation reaction at 3.5 post-Newtonian order in effective field theory*, *Phys. Rev. D* **86** (2012) 044029 [[1205.3842](#)].
- [38] C. R. Galley, *Classical Mechanics of Nonconservative Systems*, *Phys. Rev. Lett.* **110** (2013) 174301 [[1210.2745](#)].
- [39] C. R. Galley, D. Tsang and L. C. Stein, *The principle of stationary nonconservative action for classical mechanics and field theories*, [1412.3082](#).
- [40] Z. Bern, L. J. Dixon, D. C. Dunbar and D. A. Kosower, *One loop n point gauge theory amplitudes, unitarity and collinear limits*, *Nucl. Phys. B* **425** (1994) 217 [[hep-ph/9403226](#)].
- [41] Z. Bern, L. J. Dixon, D. C. Dunbar and D. A. Kosower, *Fusing gauge theory tree amplitudes into loop amplitudes*, *Nucl. Phys. B* **435** (1995) 59 [[hep-ph/9409265](#)].

- [42] R. Britto, F. Cachazo and B. Feng, *Generalized unitarity and one-loop amplitudes in  $N=4$  super-Yang-Mills*, *Nucl. Phys. B* **725** (2005) 275 [[hep-th/0412103](#)].
- [43] C. Anastasiou, R. Britto, B. Feng, Z. Kunszt and P. Mastrolia, *D-dimensional unitarity cut method*, *Phys. Lett. B* **645** (2007) 213 [[hep-ph/0609191](#)].
- [44] R. Britto and B. Feng, *Integral coefficients for one-loop amplitudes*, *JHEP* **02** (2008) 095 [[0711.4284](#)].
- [45] G. Ossola, C. G. Papadopoulos and R. Pittau, *Reducing full one-loop amplitudes to scalar integrals at the integrand level*, *Nucl. Phys. B* **763** (2007) 147 [[hep-ph/0609007](#)].
- [46] D. Forde, *Direct extraction of one-loop integral coefficients*, *Phys. Rev. D* **75** (2007) 125019 [[0704.1835](#)].
- [47] J. J. M. Carrasco, A. Edison, N. R. Del Pino and S. Zekioğlu, *An exercise in Color-Dual Cut Tiling:  $\mathcal{N} = 8$  Supergravity from Positivity*, [2408.07780](#).
- [48] Z. Bern, E. Herrmann, R. Roiban, M. S. Ruf and M. Zeng, *Global Bases for Nonplanar Loop Integrands, Generalized Unitarity, and the Double Copy to All Loop Orders*, [2408.06686](#).
- [49] G. Mogull, J. Plefka and J. Steinhoff, *Classical black hole scattering from a worldline quantum field theory*, *JHEP* **02** (2021) 048 [[2010.02865](#)].
- [50] A. Brandhuber, G. Chen, G. Travaglini and C. Wen, *A new gauge-invariant double copy for heavy-mass effective theory*, *JHEP* **07** (2021) 047 [[2104.11206](#)].
- [51] A. Edison and F. Teng, *Efficient Calculation of Crossing Symmetric BCJ Tree Numerators*, *JHEP* **12** (2020) 138 [[2005.03638](#)].
- [52] H. Frellesvig, F. Gasparotto, S. Laporta, M. K. Mandal, P. Mastrolia, L. Mattiazzi et al., *Decomposition of Feynman Integrals by Multivariate Intersection Numbers*, *JHEP* **03** (2021) 027 [[2008.04823](#)].
- [53] P. Mastrolia and S. Mizera, *Feynman Integrals and Intersection Theory*, *JHEP* **02** (2019) 139 [[1810.03818](#)].
- [54] D. Kosmopoulos, *Simplifying D-dimensional physical-state sums in gauge theory and gravity*, *Phys. Rev. D* **105** (2022) 056025 [[2009.00141](#)].
- [55] A. V. Smirnov and M. Zeng, *FIRE 6.5: Feynman integral reduction with new simplification library*, *Comput. Phys. Commun.* **302** (2024) 109261 [[2311.02370](#)].
- [56] R. A. Porto, M. M. Riva and Z. Yang, *Nonlinear Gravitational Radiation Reaction: Failed Tail, Memories & Squares*, [2409.05860](#).
- [57] D. Trestini and L. Blanchet, *Gravitational-wave tails of memory at  $4PN$  order*, in *57th Rencontres de Moriond on Gravitation*, June, 2023, [2306.00546](#).
- [58] D. Trestini and L. Blanchet, *Gravitational-wave tails of memory*, *Phys. Rev. D* **107** (2023) 104048 [[2301.09395](#)].
- [59] H. Leandro and R. Sturani, *A Gravitational non-Radiative Memory Effect*, *Gen. Rel. Grav.* **53** (2021) 26 [[2010.03119](#)].
- [60] A. Strominger and A. Zhiboedov, *Gravitational Memory, BMS Supertranslations and Soft Theorems*, *JHEP* **01** (2016) 086 [[1411.5745](#)].



- [61] A. G. Wiseman and C. M. Will, *Christodoulou’s nonlinear gravitational wave memory: Evaluation in the quadrupole approximation*, *Phys. Rev. D* **44** (1991) R2945.
- [62] K. S. Thorne, *Gravitational-wave bursts with memory: The Christodoulou effect*, *Phys. Rev. D* **45** (1992) 520.
- [63] M. Favata, *Post-Newtonian corrections to the gravitational-wave memory for quasi-circular, inspiralling compact binaries*, *Phys. Rev. D* **80** (2009) 024002 [0812.0069].
- [64] M. Favata, *The Gravitational-wave memory from eccentric binaries*, *Phys. Rev. D* **84** (2011) 124013 [1108.3121].
- [65] D. Gerosa and M. Vallisneri, *filltex: Automatic queries to ADS and INSPIRE databases to fill LaTeX bibliography*, *The Journal of Open Source Software* **2** (2017) 222.
- [66] V. A. Smirnov, *Analytic tools for Feynman integrals*, vol. 250. 2012, 10.1007/978-3-642-34886-0.
- [67] X. Liu and Y.-Q. Ma, *AMFlow: A Mathematica package for Feynman integrals computation via auxiliary mass flow*, *Comput. Phys. Commun.* **283** (2023) 108565 [2201.11669].
- [68] D. H. Bailey and D. J. Broadhurst, *Parallel integer relation detection: Techniques and applications*, *Math. Comput.* **70** (2001) 1719 [math/9905048].
- [69] A. Smirnov. <https://gitlab.com/feynmanintegrals/pslq>.
- [70] J. Klappert, F. Lange, P. Maierhöfer and J. Usovitsch, *Integral reduction with Kira 2.0 and finite field methods*, *Comput. Phys. Commun.* **266** (2021) 108024 [2008.06494].